

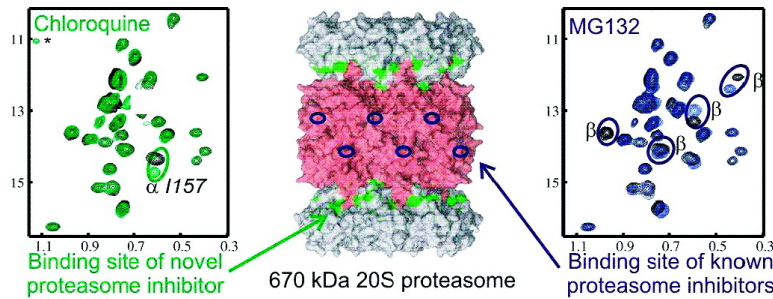
Accelerated Publication

TROSY-Based NMR Evidence for a Novel Class of 20S Proteasome Inhibitors

Remco Sprangers, Xiaoming Li, Xinliang Mao, John L. Rubinstein, Aaron D. Schimmer, and Lewis E. Kay

Biochemistry, 2008, 47 (26), 6727-6734 • DOI: 10.1021/bi8005913 • Publication Date (Web): 10 June 2008

Downloaded from <http://pubs.acs.org> on December 15, 2008



More About This Article

Additional resources and features associated with this article are available within the HTML version:

- Supporting Information
- Access to high resolution figures
- Links to articles and content related to this article
- Copyright permission to reproduce figures and/or text from this article

[View the Full Text HTML](#)



ACS Publications

High quality. High impact.

Biochemistry is published by the American Chemical Society. 1155 Sixteenth Street N.W., Washington, DC 20036

BIOCHEMISTRY

© Copyright 2008 by the American Chemical Society

Volume 47, Number 26

July 01, 2008

Accelerated Publications

TROSY-Based NMR Evidence for a Novel Class of 20S Proteasome Inhibitors[†]

Remco Sprangers,[‡] Xiaoming Li,[§] Xinliang Mao,[§] John L. Rubinstein,^{||} Aaron D. Schimmer,[§] and Lewis E. Kay*,^{*,‡}

Departments of Molecular Genetics, Biochemistry, and Chemistry, The University of Toronto, Toronto, Ontario M5S 1A8, Canada, Ontario Cancer Institute, Princess Margaret Hospital, Toronto, Ontario M5G 2M9, Canada, and Molecular Structure and Function, The Hospital for Sick Children, Toronto, Ontario M5G 1X8, Canada

Received April 4, 2008; Revised Manuscript Received May 7, 2008

ABSTRACT: The proteasome plays a central role in maintaining cellular homeostasis, in controlling the cell cycle, in removing misfolded proteins that can be toxic, and in regulating the immune system. It is also an important target for novel anticancer drugs, such as bortezomib, a potent inhibitor that has been used successfully in the treatment of multiple myeloma. Here, we show that the antimalaria drug chloroquine inhibits proteasome function in eukaryotic cell extracts and in preparations of purified 20S archaeal proteasome from *Thermoplasma acidophilum*. Methyl-TROSY-based NMR spectroscopy experiments conducted with the 670 kDa 20S proteasome localize chloroquine binding to regions between the α and β subunits of the $\alpha-\beta-\beta-\alpha$ barrel-like structure, 20 Å from the proteolytic active sites in this 7-fold symmetric molecule. Complementary amide TROSY experiments that provide further probes of proteasome–inhibitor interactions were performed on a novel 180 kDa single-ring construct containing only α subunits, the proper assembly of which was confirmed by electron microscopy. In contrast to the chloroquine–proteasome interaction described here, all previously reported inhibitors of the proteasome, including MG132, bind the catalytic region directly. Consistent with the NMR chemical shift perturbation data reported here that place chloroquine binding distal from sites of proteolysis, we show that MG132 and chloroquine can bind the proteasome simultaneously, further establishing that they exploit two completely separate binding pockets. Our data thus establish a novel class of proteasome inhibitor that functions via a mechanism distinct from binding to active sites.

The 26S proteasome is responsible for the degradation of the majority of proteins in eukaryotic cells (*1–3*). It therefore plays a critical role in regulating cellular function through

proteolysis of proteins whose activities are no longer required. The process of degradation is highly regulated and often involves ubiquitination of target molecules (*1, 3*). The 26S proteasome is comprised of a 19S regulatory particle (RP) that recognizes ubiquitin-coated proteins and a 20S core particle (CP) that contains the active sites for substrate proteolysis, localized in a central catalytic chamber that sequesters them from the cellular environment. In addition to its role in substrate recognition, the 19S particle unfolds the target in an ATP-dependent manner prior to transfer to the 20S CP. X-ray structures of the 20S CP from archaea (*4*), yeast (*5*), and bovine (*6*) show it to be composed of α

* To whom correspondence should be addressed. Phone: (416) 978-0741. Fax: (416) 978-6885. E-mail: kay@pound.med.utoronto.ca.
† This work was supported by a grant from the Canadian Institutes of Health Research (CIHR) to L.E.K. R.S. acknowledges support from the CIHR Training Program in Protein Folding and Disease. A.D.S. is a CIHR Clinician Scientist. L.E.K. is the recipient of a Canada Research Chair in Biochemistry.

‡ The University of Toronto.

§ Princess Margaret Hospital.

|| The Hospital for Sick Children.

and β rings, arranged in an $\alpha_7-\beta_7-\beta_7-\alpha_7$ configuration, giving the molecule a cylindrical shape. In the case of the CP from archaea, each of the α and β rings is comprised of a single polypeptide chain that is repeated seven times, producing heptameric rings (termed α_7 or β_7 in what follows). Catalytic activity is localized to the β subunits so that for the archaeal proteasome there are thus 14 equivalent proteolytic sites. By contrast, the 20S CPs of proteasomes from higher organisms are more complex. Here each ring is produced from seven distinct α or β subunits; only three β sites are proteolytically competent, and each has a different enzymatic activity (5).

Considering its central role in maintaining cellular homeostasis, it is not surprising that the proteasome has been implicated in the development of many human diseases (7). Moreover, because of the importance of this enzyme, in both health and disease, it was initially unanticipated that it would be a suitable drug target. In 2003, however, the FDA approved the use of the proteasome inhibitor bortezomib in the treatment of multiple myeloma (8). From a structural point of view, it is clear that this inhibitor reduces proteasome activity by binding to chymotryptic-like active sites located in the β_5 subunit (9). It remains less clear why proteasome inhibition is more toxic to tumor cells than to normal cells. Nevertheless, the anticancer activity of proteasome inhibitors has led to an increased level of interest in novel components that interfere with proteasome function, and the proteasome has emerged as a significant target in the search for cancer therapeutics.

In the development of novel inhibitors, it is often the case that initial compounds are low-affinity binders that can easily escape detection; this is problematic since localization of their sites of interaction on the target of interest is a critical first step in the drug discovery process. In this regard, NMR¹ spectroscopy is a particularly powerful technique because chemical shifts of NMR probes are exquisitely sensitive to binding events even in the millimolar range and because chemical shift perturbations can be used to map binding sites (10). This knowledge can be subsequently used to improve binding specificity and efficacy of lead compounds. An additional strength of the NMR technique relates to its ability to study interactions that involve highly dynamic components that cannot be probed in detail using other techniques. This is particularly relevant in connection with the proteasome because its substrates are unfolded polypeptide chains and because molecular dynamics are likely to be important for function. For example, in the case of the archaeal proteasome, the gating residues of the α subunits that regulate entry of substrates are known to be highly mobile (11).

Applications of NMR spectroscopy to problems in biochemistry have traditionally been limited to systems that are at least an order of magnitude smaller than the proteasome; however, a number of studies of supramolecular systems indicate that this size limit is changing (11–13). For example, recently, we have shown that very high quality $^1\text{H}-^{13}\text{C}$ methyl-TROSY (14) data sets can be recorded on a half-proteasome complex comprised of pairs of α rings, $\alpha_7-\alpha_7$, and on the full $\alpha_7-\beta_7-\beta_7-\alpha_7$ 20S CP from *Thermoplasma acidophilum* (11). Ile, Leu, and Val methyl groups from the α subunit have been assigned to specific sites in the structure, providing a large number of probes for studying molecular interactions. Although it has not been possible to record $^1\text{H}-^{15}\text{N}$ correlation maps of either $\alpha_7-\alpha_7$ or $\alpha_7-\beta_7-\beta_7-\alpha_7$ 20S CP, we show here that TROSY-based $^1\text{H}-^{15}\text{N}$ spectra (15) can be obtained for a single-ring particle, α_7 , that is stabilized through a series of mutations to the α subunit. This provides an even larger number of probes for exploring molecular interactions.

In what follows, we establish that the anti-malaria drug chloroquine inhibits proteasome function both in eukaryotic cell extracts and in the purified archaeal protein. Using $^1\text{H}-^{15}\text{N}$ (α_7) and $^1\text{H}-^{13}\text{C}$ ($\alpha_7-\alpha_7$ and $\alpha_7-\beta_7-\beta_7-\alpha_7$) TROSY-based NMR spectroscopy, we show that chloroquine specifically binds to regions at interfaces between α and β rings, distant from catalytic regions that are targeted by all other known inhibitors (16). In addition, the proteolysis pattern of α -synuclein, a 140-residue intrinsically disordered polypeptide chain, has been elucidated by two- and three-dimensional NMR spectroscopy, and it is shown that chloroquine binding to the proteasome inhibits its degradation. This study highlights the important role that solution NMR spectroscopy can play in understanding dynamic events such as substrate proteolysis and in the identification of novel, low-affinity compounds that serve as inhibitors of proteolysis that can then be subsequently refined to higher affinities at later stages of the drug discovery process.

MATERIALS AND METHODS

Enzymatic Assays. MDAY-D2 cells were lysed in 50 mM HEPES (pH 7.5), 150 mM NaCl, 1% Triton X-100, and 2 mM ATP, after which the soluble fraction was diluted to an approximate protein concentration of 10 μM with buffer A [50 mM Tris (pH 7.5) and 150 mM NaCl]. SucLLY-AMC (20 μM) and different amounts of inhibitor were added to the cell extracts. After incubation at 40 °C for 1 h, the generation of free AMC was monitored at a wavelength of 460 nm using an excitation wavelength of 380 nm. The activity of the purified TA 20S proteasome (20 nM in buffer A) was measured as described above.

NMR Spectroscopy. All protein samples were produced as described previously (11) and in the Supporting Information. NMR experiments were performed on Varian Inova 600 and 800 MHz spectrometers, equipped with cryogenically cooled and room-temperature probes, respectively. Spectra of α_7 and $\alpha_7-\alpha_7$ were recorded at 50 °C, while data sets of the full proteasome were obtained at 65 °C. NMR degradation experiments involving α -synuclein (0.1 mM substrate, 18 μM active proteasome) were performed at 5 °C, and peak intensities were extracted from a series of successively recorded HNCO data sets. Chemical shift titrations were performed at a (monomer) protein concentration of 0.3 mM, to which small volumes of chloroquine had been added, and binding constants were extracted by fitting the data to a model of independent binding (17). NMR data were processed and analyzed with nmrPipe/nmrDraw (18) with figures displaying NMR spectra and protein structures prepared using NMRview (19) and Pymol (www.delanoscientific.com), respectively.

¹ Abbreviations: NMR, nuclear magnetic resonance; TROSY, transverse relaxation-optimized spectroscopy; NOESY, nuclear Overhauser effect spectroscopy; HSQC, heteronuclear single-quantum correlation.

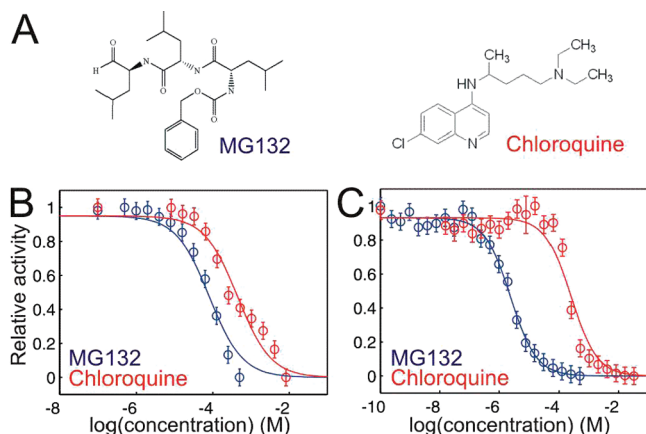


FIGURE 1: Inhibition of the 20S proteasome. (A) Structures of the proteasome inhibitors MG132 (Z-Leu-Leu-Leu-al) and chloroquine. (B) Inhibition of the 20S proteasome in MDAY-D2 cell extracts by MG132 (blue) and by chloroquine (red). (C) Inhibition of the purified 20S proteasome from *T. acidophilum* by MG132 (blue) and chloroquine (red).

RESULTS AND DISCUSSION

Chloroquine Inhibits Proteasome Activity in MDAY-D2 Cell Lines. Fluorogenic peptides, including the SucLLY-AMC peptide used here, are substrates for the proteasome and can be used to monitor proteasome activity in a straightforward manner since peptide hydrolysis is accompanied by changes in fluorescence (20). Changes in proteasome activity resulting from the addition of drug can be readily tracked through fluorescence changes, allowing for a rapid and convenient way to screen for novel components that potentially interfere with proteasome function (7, 16). Addition of the known proteasome inhibitor MG132 (Figure 1A) to cell extracts from a murine leukemia cell line (MDAY-D2) leads to decreased activity resulting from binding of MG132 to substrate recognition sites in the central catalytic chamber of the 20S CP (Figure 1B). Inhibition was also noted upon addition of chloroquine (Figures 1A,B), although higher concentrations of this compound are required (see below). Chloroquine is a widely used anti-malaria agent and recently entered clinical trials as an antiretroviral drug against HIV/AIDS (21).

Chloroquine Inhibits the Activity of Purified Proteasomes. As chloroquine is known to inhibit a number of cellular processes, including lysosomal degradation of proteins (22), we investigated whether purified proteasomes are inhibited by chloroquine as well. Here, we use the archeal proteasome from *T. acidophilum* (TA), which can be expressed in *Escherichia coli* and purified to high levels. Structurally, the archeal and eukaryotic proteasomes are very similar (2), although the former has a simpler subunit composition and is thermostable, important considerations in our NMR studies (11). Both MG132 and chloroquine indeed inhibit the purified TA proteasome (Figure 1C), although chloroquine is less efficient, as expected on the basis of studies with MDAY-D2 cell extracts described above. We are currently exploring whether synergistic effects between the two inhibitors are present.

Degradation of Cellular Protein Substrates by the 20S CP. The 20S CP can degrade intrinsically disordered proteins in an ATP-independent manner without additional “helper” molecules (23). By contrast, folded proteins are targeted for

proteolysis through the attachment of ubiquitin chains that are subsequently recognized by the 19S RP that unfolds and translocates substrates toward active sites of the CP (1, 2). α -Synuclein is one example of a naturally disordered proteasome substrate (24), and it forms the major component of Lewy bodies present in brain cells of patients with Parkinson’s disease (25). The degradation of α -synuclein has been monitored here in real time by NMR at 5 °C. This relatively low temperature was chosen to decrease enzyme activity to the point that the time dependence of hydrolysis could be followed quantitatively by two-dimensional (2D) and three-dimensional (3D) NMR spectroscopy and because spectra of α -synuclein are of higher quality at this temperature. Peak positions in NMR spectra are very sensitive to changes in protein sequence, and peaks derived from residues in the vicinity of the cleaved bond will become weaker as proteolysis progresses. Simultaneously, new resonances will appear from residues proximal to the newly formed protein termini. Figure 2A shows the ^1H – ^{15}N HSQC spectrum of α -synuclein, at 5 °C and 600 MHz, just after the addition of active proteasome (black) and after degradation has occurred for increasing amounts of time (red, green). Since each residue in α -synuclein gives rise to a single amide resonance, and since assignments of each cross-peak to specific sites in the protein are available, substrate degradation can be monitored on a per-residue basis. As expected, intensities of some of the peaks decrease significantly with time (for example, T33 and T42) (Figure 2A,B). Interestingly, however, it is clear that not all resonances of the full-length α -synuclein disappear simultaneously, suggesting that the 20S CP degrades this substrate in a sequence-dependent manner. The change in relative intensity (I/I_0 , where I is the intensity at time t and I_0 is the intensity immediately after addition of the proteasome) as a function of α -synuclein sequence is shown in Figure 2B for different incubation times. Notably, degradation at the N-terminus is fastest, while the C-terminus remains intact, even after prolonged periods of proteolysis that include incubation at 50 °C (data not shown). It is difficult to establish the exact nature of the fragments produced from the limited data recorded (HSQC and HNCO), in part because the cleavage of a peptide bond can be “sensed” by residues that are several positions removed from the site of proteolysis. It has been reported, however, that proteasome products vary in length between 3 and 30 amino acids (26). Interestingly, I_0/I' ratios (where I' is the peak intensity prior to the addition of the proteasome) establish that the C-terminus of α -synuclein associates with the proteasome to a greater extent than other regions of the substrate (Figure 2C) that likely reflects very transient binding since we have not been able to observe the corresponding changes on the proteasome. Although it is tempting to speculate that binding at the C-terminus correlates with preferential degradation of the N-terminal part of the protein, it is likely that the difference in cleavage reflects sequence-specific effects, resulting perhaps from the large number of negatively charged residues at the C-terminus of α -synuclein. Upon addition of chloroquine, degradation of α -synuclein is slowed dramatically (Figure 2D), establishing that this compound inhibits not only proteasomal degradation of model peptides but also the degradation of disordered protein substrates.

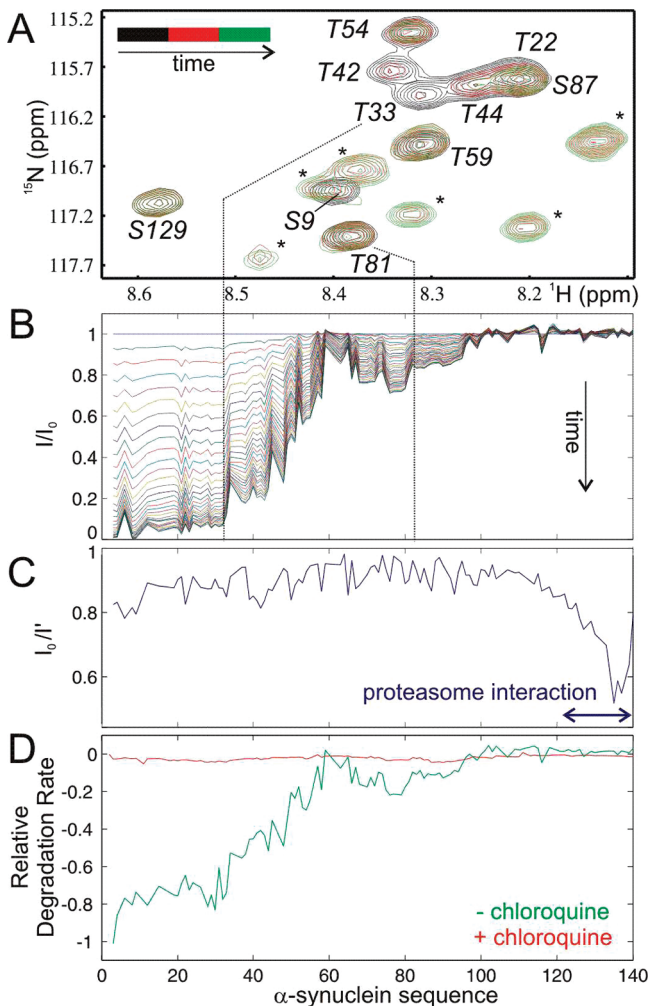


FIGURE 2: Degradation of α -synuclein by the proteasome. (A) Overlay of ^1H - ^{15}N HSQC spectra of α -synuclein (5°C) immediately after the addition of the proteasome (black) and after degradation for 60 (red) and 120 h (green). Assignments of correlations of the intact α -synuclein are indicated, and peaks labeled with asterisks derive from degradation products and increase in magnitude with time. (B) Relative intensities of α -synuclein correlations over time, as extracted from a series of HNCO experiments. (C) Intensities of α -synuclein cross-peaks immediately after the addition of the active proteasome (I_0) relative to intensities in the absence of enzyme (I'). (D) Relative rates of degradation of α -synuclein in the absence (green) and presence (red) of 25 mM chloroquine, at 5°C (250 μM proteasome in monomer). The relative rate equals the slope of peak intensity vs time, normalized such that the maximum rate is -1 . Addition of chloroquine slows degradation by a factor of at least 20.

Mapping Binding of Chloroquine on the 20S CP and on $\alpha_7-\alpha_7$ by Methyl-TROSY To gain insight into the structural basis of proteasome inhibition by chloroquine, we turn to methyl-TROSY NMR spectroscopy of highly deuterated protein samples that are labeled with ^{13}C and ^1H in methyl positions of Ile- $\delta 1$, Leu, and Val (only one of the two prochiral methyls is labeled). We have recently shown that very high quality data sets can be recorded on the 670 kDa 20S CP (Figure 3A, bottom) using this methodology (11), allowing, for example, the site-specific detection of drug binding through monitoring changes in chemical shifts. The top panel of Figure 3A shows a portion of the ^1H - ^{13}C Ile- $\delta 1$ -[$^{13}\text{CH}_3$], Leu, Val-[$^{13}\text{CH}_3$, $^{12}\text{CD}_3$] methyl TROSY spectrum of the 20S CP, at 65°C and 800 MHz, that is isotopically enriched in both α and β subunits (black

spectrum). Addition of chloroquine clearly changes the position of a select number of resonances in the spectrum (red), indicating a specific drug–enzyme interaction. As described previously, site-specific assignments are available for Ile, Leu, and Val methyl groups of the α subunits of the 20S CP; cross-peaks from α that are perturbed upon addition of inhibitor are labeled, while those derived from β are denoted with β . The changes are confirmed in Figure 3B that shows the same spectral region of a ^1H - ^{13}C methyl TROSY spectrum of the 20S CP recorded on a sample that is isotopically enriched only in the α subunits. Interestingly, residues in both the outer α and in the inner β rings are affected by chloroquine (Figure 3A, top), consistent with binding occurring in a region at the interface of the α - β rings. This is confirmed by assignments of the methyl groups of the α ring that show that those methyls that are affected by inhibitor are proximal to the β subunits. From the change in chemical shift upon subsequent additions of chloroquine to the 20S CP, a dissociation constant of $560 \pm 100 \mu\text{M}$ is obtained (Figure 3B, bottom).

Due to the absence of some resonances at the α - β interface in spectra of the full proteasome (11), we decided to use a simpler construct that produces higher-quality spectra. As reported previously (11, 27), the proteasome α subunits spontaneously assemble into 360 kDa “half-proteasome” particles, $\alpha_7-\alpha_7$ (Figure 3A, bottom), for which we also have previously reported methyl group chemical shift assignments. Addition of chloroquine to the half-proteasome results in chemical shift perturbations of residues that would normally be located close to the β ring interface in the intact 20S CP (Figure 3C) (50°C). As expected, additional residues that are affected by inhibitor binding could be identified relative to the case for the 20S CP. However, chloroquine binding to $\alpha_7-\alpha_7$ is more than an order of magnitude weaker (Figure 3C, bottom), indicating that the β subunits do play an important role in stabilizing the chloroquine–proteasome interaction.

Probing the Chloroquine–Proteasome Interaction by ^1H - ^{15}N TROSY of a 180 kDa Single-Ring Particle. The major advantage of methyl-TROSY in relation to other NMR approaches for studies of supramolecular systems is one of sensitivity. However, on average, Ile, Leu, and Val comprise only $\approx 20\%$ of the residues in a protein, and in many cases, it would be advantageous to increase the number of probes available. In addition, chemical shift perturbations in methyl spectra upon addition of ligand can be quite small, often less than a line width for chloroquine. Ideally, one would like to supplement the methyl data with additional information obtained from backbone amide groups that are, in general, very sensitive to the addition of ligands. However, we have not been able to record reasonable ^1H - ^{15}N correlation spectra of either the 20S CP or $\alpha_7-\alpha_7$. We therefore dissected the proteasome further through mutagenesis in an attempt to prepare smaller particles that would be within the “range” of ^1H - ^{15}N TROSY-HSQC experiments (15). Deletion of residues 97–103 from the native α subunit sequence prevented formation of $\alpha_7-\alpha_7$ and produced a single-ring structure, α_7 (180 kDa), with the same 7-fold symmetry as the full proteasome as determined using negative stain electron microscopy (Supporting Information, Figure S1). High-quality ^1H - ^{15}N correlation maps could now be obtained, although only 3D HNCO and HNCA triple-resonance

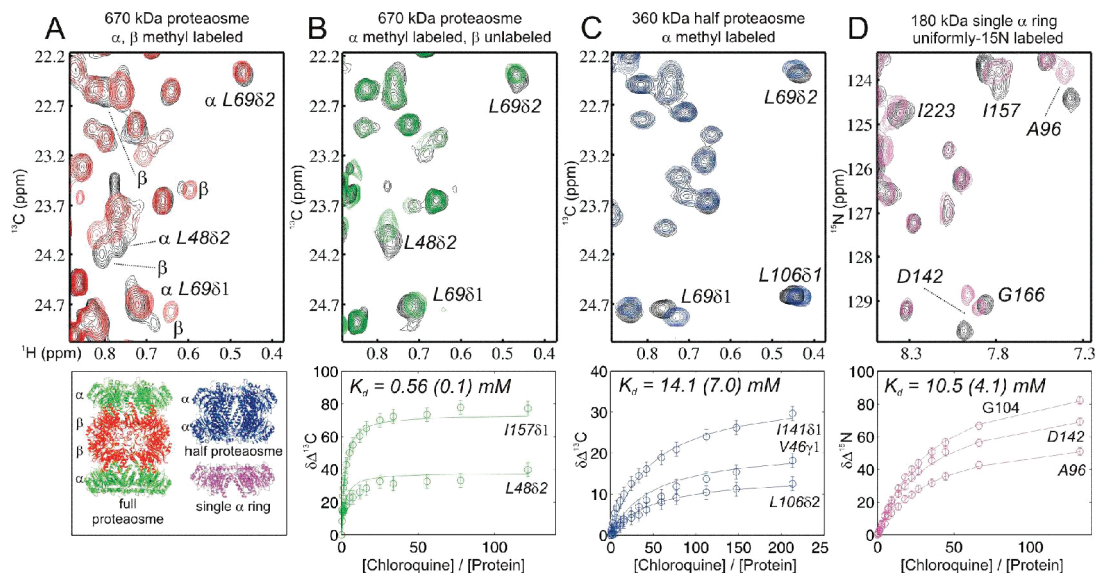


FIGURE 3: Mapping the binding of chloroquine on the 20S proteasome. (A) Spectra of uniformly Ile- δ 1-[$^{13}\text{CH}_3$], Leu, Val-[$^{13}\text{CH}_3, ^{12}\text{CD}_3$]-labeled proteasome before (black) and after (red) addition of chloroquine, at 65 °C, 800 MHz. Resonances originating from the α and β subunits that are affected by binding are labeled. Chemical shift assignments are indicated for correlations derived from residues in α chains. The bottom panel shows structures of the molecules analyzed (4). (B) As in panel A with only the α subunits labeled and where contours in green correspond to those after addition of saturating amounts of chloroquine. The bottom panel shows ^{13}C chemical shift changes of selected peaks vs [inhibitor]_{total}/[protein]_{total}; a K_D value of 0.56 ± 0.1 mM is extracted. (C) Spectra of a uniformly Ile- δ 1-[$^{13}\text{CH}_3$], Leu, Val-[$^{13}\text{CH}_3, ^{12}\text{CD}_3$]-labeled half-proteasome in the absence (black) and presence (blue) of chloroquine, at 50 °C, 800 MHz. Assignments of the residues affected by chloroquine are indicated. The bottom panel shows titration curves as in panel B. (D) Spectra of a uniformly ^{15}N - and ^2H -labeled single- α ring without (black) and with (red) chloroquine, at 50 °C, 600 MHz. Assignments for residues that are affected by chloroquine are indicated. The bottom panel shows titration curves as in panels B and C.

experiments were feasible. By comparing 3D HNCA and ^{15}N -edited NOESY data sets recorded on α_7 with corresponding spectra for a monomeric α species that was also produced by mutagenesis and for which near-complete assignments were available (11), we were able to assign $\approx 95\%$ of the *observed* correlations in the α_7 ^1H - ^{15}N map. However, for approximately one-third of the residues in the single ring it was not possible to observe correlations in ^1H - ^{15}N -based spectra (Supporting Information, Figure S2). Interestingly, some of these missing cross-peaks are from residues located in regions of the protein that could be quantified by methyl-TROSY and have been identified as undergoing chemical exchange on the millisecond time scale or localized to regions that have extensive picosecond to nanosecond time scale dynamics (Supporting Information, Figure S3). Thus, ^{15}N - and ^{13}C -based spectra are very much complementary and should always be recorded in the study of the structure, dynamics, and interactions of supramolecular systems, if possible. Addition of chloroquine to the single- α ring produces a subset of chemical shift changes that derive from residues localized in regions that are consistent with expectations based on ^1H - ^{13}C methyl data (Figure 3D); moreover, several additional residues could be identified since ^{15}N probes at every site are available. Chemical shift titration data establish that the affinities of chloroquine for α_7 (Figure 3D, bottom) and for $\alpha_7-\alpha_7$ (Figure 3C, bottom) are comparable. In principle, it would be of interest to extend this analysis to include titration studies of the α monomer. However, the monomeric form is stabilized through the addition of a significant number of mutations ($\Delta 2-34$, R57A, R86A, and R130A) (11), and it may well be difficult to separate the effects of mutations from intrinsic differences in binding between wild-type monomeric and oligomeric α

states. We have therefore chosen not to study the chloroquine α monomer interaction.

Chloroquine Binds to a Negatively Charged Region at the $\alpha-\beta$ Interface. ^1H - ^{13}C methyl-TROSY spectra of the 20S CP and $\alpha_7-\alpha_7$ as well as ^1H - ^{15}N data sets of α_7 consistently show that residues in the α subunits that are close to the $\alpha-\beta$ interface are affected by chloroquine binding (Figure 4A,B, residues highlighted in green; Table S1). Interestingly, the mapped interaction site is large compared to the size of the drug, perhaps due to the aromatic nature of the inhibitor (Figure 1A) that causes chemical shift changes distant from the binding site due to ring current effects. Alternatively, a conformational change might occur in the proteasome that leads to chemical shift changes in regions that are removed from the direct site of interaction. The changes, nevertheless, localize to protrusions in the α subunit (Figure 4B) that bind to corresponding grooves in the β subunit, fitting together in a lock-key type manner (Figure 4A). Notably, chemical shift changes occur in a region of the proteasome that has a negative surface potential (Figure 4C). Interestingly, it has recently been shown that chloroquine interferes with the potassium channel Kir.2.1 through interactions that are mediated by a negative surface area in the channel (28). In addition, the lactate dehydrogenase structure from the malaria-causing parasite *Plasmodium falciparum* in complex with chloroquine shows that the drug is stabilized by hydrogen bonds to a pair of acidic residues in the protein (29). It may be that a similar network of hydrogen bonds plays a role in stabilizing the drug- α subunit interaction. It is noteworthy that the negative surface charge is conserved between the TA proteasome and most of the seven different α subunits in the eukaryotic proteasome. A more detailed description of the substrate-proteasome interaction must

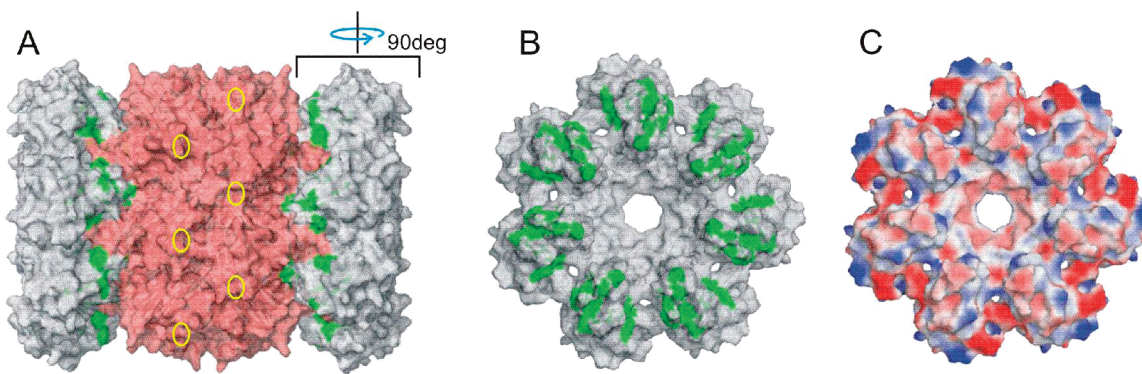


FIGURE 4: Binding site of chloroquine on the proteasome. (A) Structure of the proteasome with residues showing chemical shift changes upon addition of chloroquine colored green. The α subunits are colored gray and the β subunits red; active site threonines are located inside the catalytic chamber below the yellow circles. Distances from chloroquine binding $\alpha-\beta$ interfaces to the active sites are 20 Å. (B) The α ring is flipped open, allowing a view of the inside of the antechamber. The substrate enters the proteasome via the gate, visible in the back. (C) Electrostatic surface potential of the inside of the α ring (same view as in panel B). Chloroquine interacts predominantly with a negatively charged region.

await a high-resolution crystal structure of the complex that we are currently attempting to produce.

Chloroquine Binding Is Structurally Distinct from Interactions of Other Inhibitors. With the exception of chloroquine, all known drugs that inhibit proteasome function bind at or close to the active sites of the β subunits that localize to the lumen of the enzyme barrel (16). Figure 5A shows the Ile region of the $^1\text{H}-^{13}\text{C}$ methyl-TROSY spectrum of the 20S CP with both α and β subunits labeled (black) and the changes that accompany the addition of saturating amounts of the commonly used proteasome inhibitor MG132 (blue). Only residues in the β rings are affected by drug binding, as expected from structural studies of a homologous inhibitor that shows binding to the substrate recognition groove close to the active site threonine (4). By contrast, we have established here that chloroquine binds to regions between the α and β rings (Figures 3A,B, 4A,B, and 5B), and a comparison of panels A and B of Figure 5 clearly shows that a different subset of residues is affected by binding of the two inhibitors. This strongly suggests that the binding regions are isolated so that both inhibitors can bind to the proteasome simultaneously. Indeed, addition of a mixture of MG132 and chloroquine to the 20S CP results in chemical shift changes that are a simple addition of those that accompany binding of inhibitors when added separately (Figure 5C). This provides very strong evidence that chloroquine modulates proteasomal activity by a mechanism distinct from direct interaction with residues near or at the active sites. It may be that chloroquine interferes with substrate translocation or that its binding induces an allosteric effect that is transmitted to the sites of proteolysis. Consistent with the discussion given above is the fact that the proteasome activity data of Figure 1C (red) can be fit to a noncompetitive inhibition model of binding with a K_1 of 0.27 ± 0.05 mM that is in agreement with the K_D from chemical shift titrations [0.56 ± 0.1 mM (Figure 3B)]; small differences between K_1 and K_D likely reflect the different conditions used for both sets of experiments (40°C vs 65°C , ^1H -labeled vs ^2H -labeled proteasome, and H_2O vs D_2O). As an interesting aside, one Ile residue from the β subunit that shifts in the presence of MG132 (boxed region, Figure 5C) also shifts upon addition of the substrate α -synuclein to the uninhibited proteasome (Figure 5D). As shown in Figure 2, α -synuclein is degraded by the proteasome over time, and the cross-peak

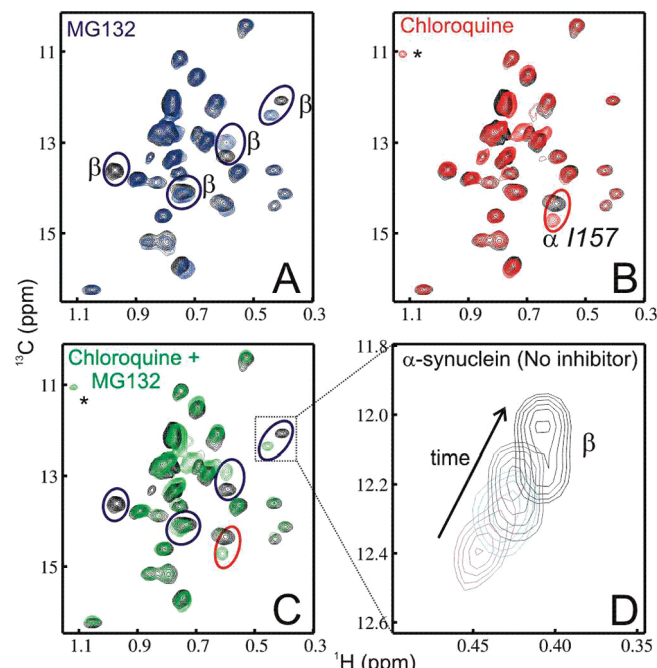


FIGURE 5: Active site inhibitor MG132 and chloroquine bind the proteasome by independent mechanisms. (A–C) Ile region of the $^1\text{H}-^{13}\text{C}$ spectrum of the full proteasome, methyl labeled in both α and β subunits in the absence (black) and presence of inhibitors MG132 (A, blue), chloroquine (B, red), or both (C, green). Correlations in the α subunit that shift upon binding of the inhibitor are indicated, with β denoting cross-peaks from residues in the β subunit (unassigned). Resonances indicated with an asterisk derive from a methyl group in chloroquine (Figure 1A). (D) Resonance in the box of panel C affected by MG132 and by the substrate α -synuclein (in the absence of inhibitor). Immediately after addition of α -synuclein, a correlation in red is observed that evolves back to the free state (black) over time due to substrate degradation, as indicated by the arrow. The large line width in the carbon dimension results from $^{13}\text{C}-^{13}\text{C}$ one-bond couplings due to ^{13}C enrichment in both the Ile- $\delta 1$ and Ile- $\gamma 1$ atoms in this particular sample.

from this Ile moves back to its original position in the free proteasome as substrate is consumed and product is released (red to black, denoted by the arrow in Figure 5D). This cross-peak can be assigned with high probability to β -Ile45 that lines the substrate specificity pocket.

Search for Proteasome Inhibitors. Chloroquine has a long history as a drug against malaria. It has been used to treat a variety of autoimmune disorders, and it is a potential antiviral

drug against HIV/AIDS (21). Although chloroquine is known to inhibit protein degradation through disruption of lysosomal function (22), to the best of our knowledge its inhibition of the proteasome has not been reported and perhaps for good reason. Assuming a total protein concentration of 300 mg/mL in the cell, of which $\approx 1\%$ ($4 \mu\text{M}$) is the proteasome (30, 31), the amount of chloroquine required to significantly inhibit the proteasome is greater than the clinical range, as lethal poisoning occurs at blood concentrations of $> 40 \mu\text{M}$ (32). Although it is unlikely that chloroquine will be clinically relevant as a proteasome inhibitor, the study of its interaction with the 20S CP reported here is significant because it establishes that it is possible to inhibit proteasome function in a novel way through binding to sites that are distinct from those occupied by previously described inhibitors. Since the introduction of bortezomib, the search for new proteasome inhibitors that have anticancer function has intensified, and to date, efforts have focused on inhibitors that directly bind the catalytic regions of the enzyme (16). The discovery of new sites on the protein that can be targeted for inhibition is important for further drug development. It is clear that in this context simple but powerful NMR experiments can play a significant role.

ACKNOWLEDGMENT

Dr. Julie Forman-Kay (The Hospital for Sick Children) is thanked for providing laboratory space and Dr. Ranjith Muhandiram for help with NMR experiments. The expression construct of α -synuclein was a kind gift of Dr. P. Thomas (University of Texas Southwestern Medical Center, Dallas, TX). This work is dedicated to the memory of my friend Richard Lewis who succumbed to AML in May 2007 (L.E.K.).

SUPPORTING INFORMATION AVAILABLE

Description of protein cloning, expression, and purification, figures showing an EM image of α_7 , the $^1\text{H}-^{15}\text{N}$ NMR spectrum of α_7 , and regions on the α ring where amide correlations could not be observed in spectra, and one table listing residues whose shifts are affected by binding of chloroquine. This material is available free of charge via the Internet at <http://pubs.acs.org>.

REFERENCES

- Goldberg, A. L. (2003) Protein degradation and protection against misfolded or damaged proteins. *Nature* **426**, 895–899.
- Baumeister, W., Walz, J., Zuhl, F., and Seemuller, E. (1998) The proteasome: Paradigm of a self-compartmentalizing protease. *Cell* **92**, 367–380.
- Pickart, C. M., and Cohen, R. E. (2004) Proteasomes and their kin: Proteases in the machine age. *Nat. Rev. Mol. Cell Biol.* **5**, 177–187.
- Lowe, J., Stock, D., Jap, B., Zwickl, P., Baumeister, W., and Huber, R. (1995) Crystal structure of the 20S proteasome from the archaeon *T. acidophilum* at 3.4 Å resolution. *Science* **268**, 533–539.
- Groll, M., Ditzel, L., Lowe, J., Stock, D., Bochtler, M., Bartunik, H. D., and Huber, R. (1997) Structure of 20S proteasome from yeast at 2.4 Å resolution. *Nature* **386**, 463–471.
- Unno, M., Mizushima, T., Morimoto, Y., Tomisugi, Y., Tanaka, K., Yasuoka, N., and Tsukihara, T. (2002) The structure of the mammalian 20S proteasome at 2.75 Å resolution. *Structure* **10**, 609–618.
- Kisselev, A. F., and Goldberg, A. L. (2001) Proteasome inhibitors: From research tools to drug candidates. *Chem. Biol.* **8**, 739–758.
- Richardson, P. G., Sonneveld, P., Schuster, M. W., Irwin, D., Stadtmauer, E. A., Facon, T., Harousseau, J. L., Ben-Yehuda, D., Lonial, S., Goldschmidt, H., Reece, D., San-Miguel, J. F., Blade, J., Boccadoro, M., Cavenagh, J., Dalton, W. S., Boral, A. L., Esseltine, D. L., Porter, J. B., Schenkein, D., and Anderson, K. C. (2005) Bortezomib or high-dose dexamethasone for relapsed multiple myeloma. *N. Engl. J. Med.* **352**, 2487–2498.
- Groll, M., Berkers, C. R., Ploegh, H. L., and Ovaa, H. (2006) Crystal structure of the boronic acid-based proteasome inhibitor bortezomib in complex with the yeast 20S proteasome. *Structure* **14**, 451–456.
- Shuker, S. B., Hajduk, P. J., Meadows, R. P., and Fesik, S. W. (1996) Discovering high-affinity ligands for proteins: SAR by NMR. *Science* **274**, 1531–1534.
- Sprangers, R., and Kay, L. E. (2007) Quantitative dynamics and binding studies of the 20S proteasome by NMR. *Nature* **445**, 618–622.
- Fiaux, J., Bertelsen, E. B., Horwich, A. L., and Wuthrich, K. (2002) NMR analysis of a 900K GroEL GroES complex. *Nature* **418**, 207–211.
- Gelis, I., Bonvin, A. M., Keramisanou, D., Koukaki, M., Gouridis, G., Karamanou, S., Economou, A., and Kalodimos, C. G. (2007) Structural basis for signal-sequence recognition by the translocase motor SecA as determined by NMR. *Cell* **131**, 756–769.
- Tugarinov, V., Hwang, P. M., Ollerenshaw, J. E., and Kay, L. E. (2003) Cross-correlated relaxation enhanced $^1\text{H}-^{13}\text{C}$ NMR spectroscopy of methyl groups in very high molecular weight proteins and protein complexes. *J. Am. Chem. Soc.* **125**, 10420–10428.
- Pervushin, K., Riek, R., Wider, G., and Wuthrich, K. (1997) Attenuated T2 relaxation by mutual cancellation of dipole-dipole coupling and chemical shift anisotropy indicates an avenue to NMR structures of very large biological macromolecules in solution. *Proc. Natl. Acad. Sci. U.S.A.* **94**, 12366–12371.
- Borissenko, L., and Groll, M. (2007) 20S proteasome and its inhibitors: Crystallographic knowledge for drug development. *Chem. Rev.* **107**, 687–717.
- Johnson, P. E., Tomme, P., Joshi, M. D., and McIntosh, L. P. (1996) Interaction of soluble cellooligosaccharides with the N-terminal cellulose-binding domain of *Cellulomonas fimi* CenC 2. NMR and ultraviolet absorption spectroscopy. *Biochemistry* **35**, 13895–13906.
- Delaglio, F., Grzesiek, S., Vuister, G. W., Zhu, G., Pfeifer, J., and Bax, A. (1995) NMRPipe: A multidimensional spectral processing system based on UNIX pipes. *J. Biomol. NMR* **6**, 277–293.
- Johnson, B. A. (2004) Using NMRView to visualize and analyze the NMR spectra of macromolecules. *Methods Mol. Biol.* **278**, 313–352.
- Rock, K. L., Gramm, C., Rothstein, L., Clark, K., Stein, R., Dick, L., Hwang, D., and Goldberg, A. L. (1994) Inhibitors of the proteasome block the degradation of most cell proteins and the generation of peptides presented on MHC class I molecules. *Cell* **78**, 761–771.
- Savarino, A., Boelaert, J. R., Cassone, A., Majori, G., and Cauda, R. (2003) Effects of chloroquine on viral infections: An old drug against today's diseases? *Lancet Infect. Dis.* **3**, 722–727.
- de Duve, C., de Barsy, T., Poole, B., Trouet, A., Tulkens, P., and Van Hoof, F. (1974) Commentary. Lysosomotropic agents. *Biochem. Pharmacol.* **23**, 2495–2531.
- Tofaris, G. K., Layfield, R., and Spillantini, M. G. (2001) α -Synuclein metabolism and aggregation is linked to ubiquitin-independent degradation by the proteasome. *FEBS Lett.* **509**, 22–26.
- Eliezer, D., Kutluay, E., Bussell, R., Jr., and Browne, G. (2001) Conformational properties of α -synuclein in its free and lipid-associated states. *J. Mol. Biol.* **307**, 1061–1073.
- Spillantini, M. G., Schmidt, M. L., Lee, V. M., Trojanowski, J. Q., Jakes, R., and Goedert, M. (1997) α -Synuclein in Lewy bodies. *Nature* **388**, 839–840.
- Kisselev, A. F., Akopian, T. N., and Goldberg, A. L. (1998) Range of sizes of peptide products generated during degradation of different proteins by archaeal proteasomes. *J. Biol. Chem.* **273**, 1982–1989.
- Zwickl, P., Kleinz, J., and Baumeister, W. (1994) Critical elements in proteasome assembly. *Nat. Struct. Biol.* **1**, 765–770.
- Rodriguez-Menchaca, A. A., Navarro-Polanco, R. A., Ferrer-Villada, T., Rupp, J., Sachse, F. B., Tristani-Firouzi, M., and Sanchez-Chapula, J. A. (2008) The molecular basis of chloroquine

- block of the inward rectifier Kir2.1 channel. *Proc. Natl. Acad. Sci. U.S.A.* **105**, 1364–1368.
29. Read, J. A., Wilkinson, K. W., Tranter, R., Sessions, R. B., and Brady, R. L. (1999) Chloroquine binds in the cofactor binding site of *Plasmodium falciparum* lactate dehydrogenase. *J. Biol. Chem.* **274**, 10213–10218.
30. Pollard, T., and Earnshaw, W. (2004) *Cell Biology*, 2nd ed., Sanders Elsevier, New York.
31. Tanaka, K., Ii, K., Ichihara, A., Waxman, L., and Goldberg, A. L. (1986) A high molecular weight protease in the cytosol of rat liver. I. Purification, enzymological properties, and tissue distribution. *J. Biol. Chem.* **261**, 15197–15203.
32. Riou, B., Barriot, P., Rimailho, A., and Baud, F. J. (1988) Treatment of severe chloroquine poisoning. *N. Engl. J. Med.* **318**, 1–6.

BI8005913

Supporting Information

TROSY-based NMR evidence for a novel class of 20S proteasome inhibitor

Remco Sprangers, Xiaoming Liqq, Xinliang Mao, John L. Rubinstein, Aaron D.

Schimmer and Lewis E. Kay

Supporting Methods

Protein Cloning, Expression and Purification. The monomeric α ring, denoted by α_7 in the text, has been constructed by deleting residues 97 to 103 from the native protein sequence, using conventional cloning techniques. The 20S proteasome was expressed as described previously (1). Briefly, the α and β subunits were either co-expressed from one plasmid (where the β subunit carried a C-terminal His6-tag), co-expressed from 2 different plasmids (where the α subunit contained a TEV cleavable N-terminal His6-tag) or both subunits were expressed separately (with a TEV cleavable His6-tag on each of the subunits). Methyl labeling of proteins was achieved by growing cells in D_2O based minimal medium with 2H - ^{12}C glucose as the carbon source. One hour before induction of protein expression, α -ketobutyric acid (60 mg/liter) and α -ketoisovaleric acid (100 mg/liter; only one of the two isopropyl methyls was $^{13}CH_3$ labeled, the other $^{12}CD_3$) were added to introduce $^{13}CH_3$ methyl groups in Ile, Leu and Val (2). Proteins were purified by Ni-NTA affinity resin and size exclusion chromatography. Proteasomes only isotopically enriched in the α subunits were reconstituted by mixing separately expressed α and β subunits followed by an additional size exclusion purification step. Highly deuterated,

¹⁵N/ ¹³C¹⁵N labeled α_7 samples were prepared after first dialyzing the GuHCl (6.0 M) denatured protein against a non-denaturing buffer. NMR samples were typically 300 μ M in total proteasome (monomer concentration) in 100% D₂O (¹³C labeling), 25 mM potassium phosphate pH 6.8, 50 mM NaCl, 1 mM EDTA, 0.03% NaN₃ and 2 mM DTT or in 90%H₂O/10%D₂O ([α_7]; ¹⁵N/ ¹³C¹⁵N labeling) with the same buffer composition as above.

Electron Microscopy. Purified α rings (4 μ L) at a concentration of 5 μ g/mL were applied to the surface of a continuous carbon film coated electron microscopy (EM) grid that had been previously made hydrophilic by glow discharge in air. Protein was allowed to adsorb to the carbon surface for 2 min. The grid was washed once with water (50 μ L) and stained with 2 % (w/v) uranyl acetate (50 μ L). The grid was imaged with a FEI F20 microscope (FEI Company, Eindhoven, Netherlands) operating at 200 kV with a magnification of 50,000 x and a defocus of 0.5 μ m. Images were recorded on Kodak SO-163 film, developed in full strength D19 solution for 12 minutes and digitized with an Intergraph Photoscan densitometer (Intergraph, Huntsville, Alabama, USA) using a 7 μ m step size. Pixels were averaged 3 x 3 to give an effective pixel size of 4.2 x 4.2 \AA . 1000 particle images were selected interactively, band pass filtered between 700 and 20 \AA with a modified Gaussian edge filter and subjected to reference-free alignment with SPIDER (3). Symmetry was not applied during the alignment and averaging. Multivariate statistical analysis with SPIDER failed to provide evidence of any symmetry besides a 7-fold rotation axis.

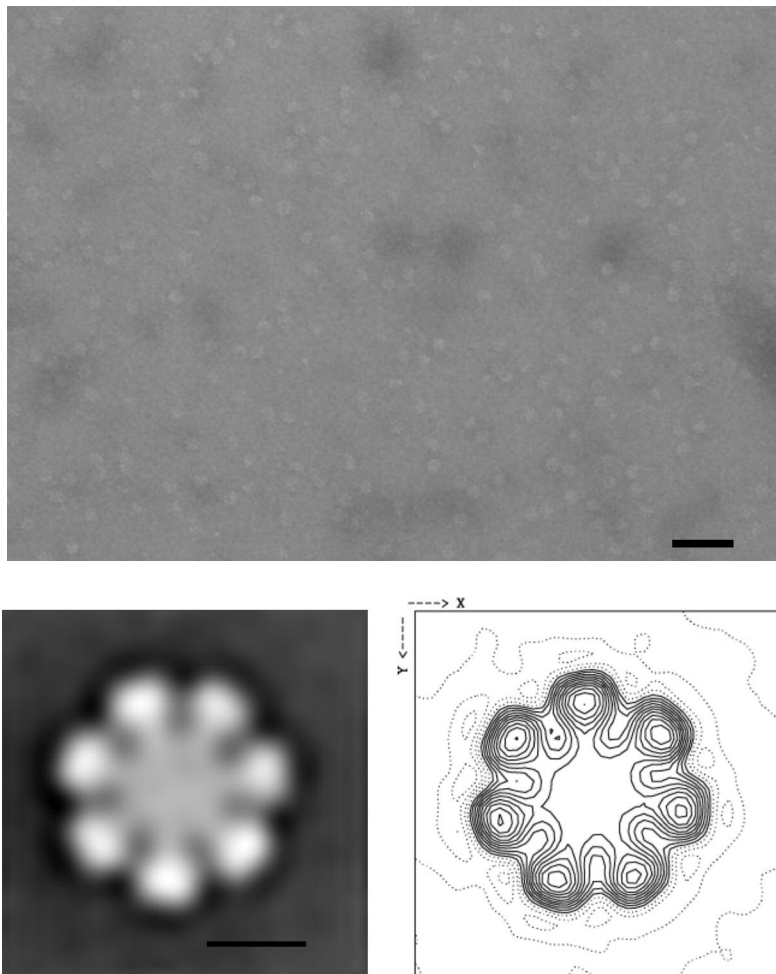


Figure S1. Top: Sample region of an EM micrograph. The scale bar represents 500 Å.
Bottom: An average of 1000 aligned images of proteasome α rings and corresponding contour map. The scale bar represents 50 Å.

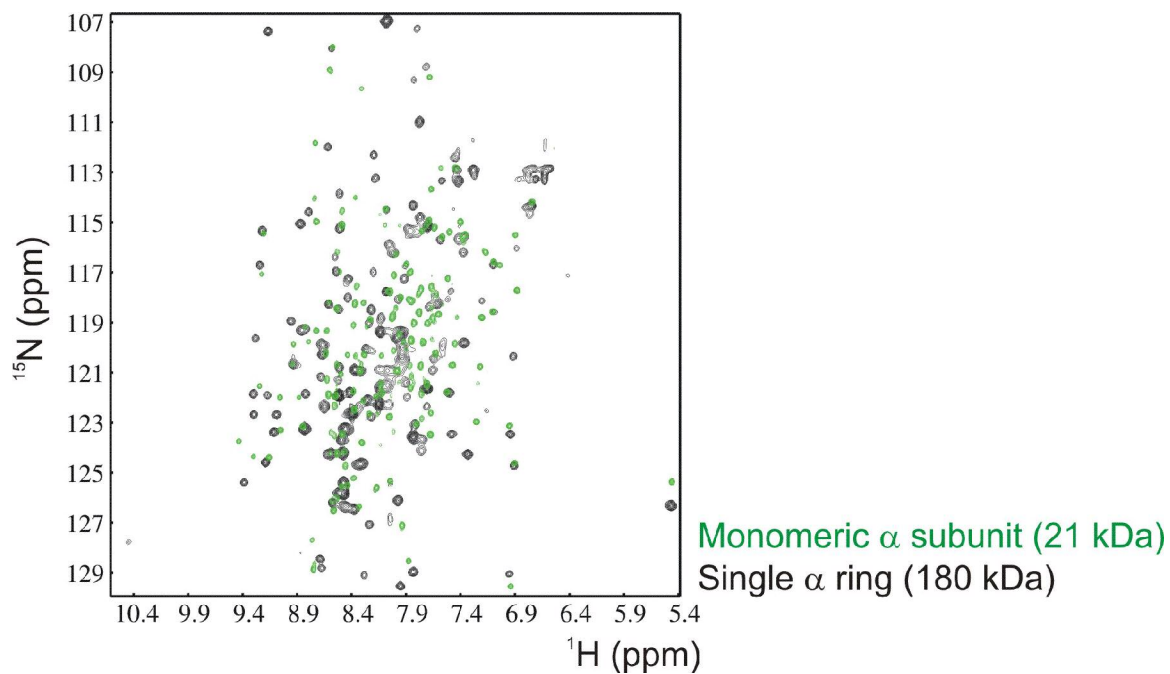


Figure S2. Overlay of the ^1H - ^{15}N TROSY-HSQC spectra of α_7 (180 kDa, black) with the monomeric alpha subunit (21 kDa, green), 50°C, 600 MHz. A direct transfer of assignments from the spectrum of the single subunit to the spectrum of α_7 is not possible; however, shifts between the two forms are small in many cases.

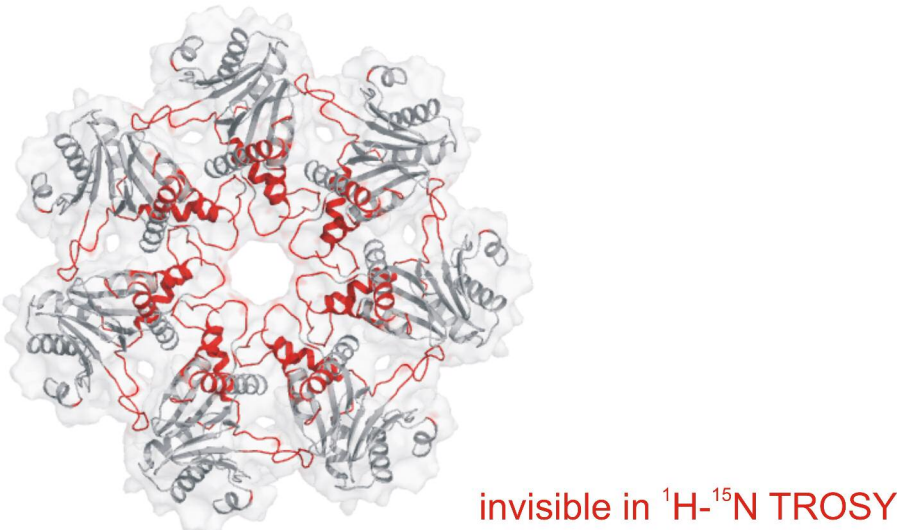


Figure S3. Regions of the single α ring that are not visible in ^1H - ^{15}N based spectra. The ‘invisible’ region include residues that undergo ms timescale motions and that can be observed in ^1H - ^{13}C methyl-TROSY data sets, illustrating the complementarily of ^{15}N and ^{13}C -based experiments.

Table S1. Residues Whose Chemical Shifts are Affected by Chloroquine Binding

^1H - ^{13}C Methyl TROSY (full proteasome):
Leu 48, Leu 69, Ile 157, Val 217, Ile 223

^1H - ^{13}C Methyl TROSY ($\alpha 7\alpha 7$):
Val 46, Ile 67, Leu 69, Val 101, Leu 106, Val 107, Ile 141, Ile 144, Val 217, Ile 223

^1H - ^{15}N Amide TROSY ($\alpha 7$):
Ala 92, Arg 93, Ala 96, Gly 104, Ile 109, Leu 112, Gly 140, Asp 142, Gly 145, Cys 151, Ile 157, Gly 166, Tyr 221, Ile 223

Supporting References

1. Sprangers, R. & Kay, L. E. (2007) Quantitative dynamics and binding studies of the 20S proteasome by NMR *Nature*. 445: 618-22.
2. Goto, N. K., Gardner, K. H., Mueller, G. A., Willis, R. C. & Kay, L. E. (1999) A robust and cost-effective method for the production of Val, Leu, Ile (delta 1) methyl-protonated ¹⁵N-, ¹³C-, ²H-labeled proteins *J Biomol NMR*. 13: 369-74.
3. Frank, J., et al. (1996) SPIDER and WEB: processing and visualization of images in 3D electron microscopy and related fields *J Struct Biol* 116: 190-9.